ISSN 2070-2051, Protection of Metals and Physical Chemistry of Surfaces, 2014, Vol. 50, No. 7, pp. 875–882. © Pleiades Publishing, Ltd., 2014.
Original Russian Text © I.V. Petukhov, N.A. Medvedeva, I.R. Subakova, V.I. Kichigin, 2013, published in Korroziya: Materialy, Zashchita, 2013, No. 1, pp. 36–43.

PROTECTIVE COATINGS

Corrosion-Electrochemical Behavior of Ni–P Coatings in Deaerated Acidic Sulfate Solutions

I. V. Petukhov, N. A. Medvedeva, I. R. Subakova, and V. I. Kichigin

Perm State University, Perm, Russia

e-mail: Petukhov-309@yandex.ru

Received June 25, 2012

Abstract—The corrosion-electrochemical behavior of Ni–P coatings in acidic sulfate solutions (a pH of 0.5–2.0) has been studied. It has been found that the hydrogen evolution reaction occurs through the discharge–electrochemical desorption route. Ni–P coatings are more efficient cathode materials in acidic sulfate media than nickel is. Preliminary cathodic polarization and an inert atmosphere have little effect on the behavior of the polarization curves of Ni–P coatings containing 13.4% phosphorus and significantly accelerate the anodic dissolution of coatings containing 8.0 and 11.1% phosphorus.

Keywords: Ni–P coatings, corrosion-electrochemical behavior, hydrogen evolution reaction

DOI: 10.1134/S2070205114070144

INTRODUCTION

Nickel–phosphorous coatings are extensively used, partly they exhibit a fairly high corrosion resistance in various media. The corrosion resistance and anodic dissolution of Ni–P coatings has been the subject of many studies [1–5]. In particular, it has been found that amorphous Ni–P coatings (with a high phosphorus content) exhibit a higher corrosion resistance than do crystalline coatings with a low phosphorus content. Unlike nickel, during anodic polarization, Ni–P coatings do not undergo passivation [4, 5].

It is believed that anodic dissolution is accompanied by preferred dissolution of nickel and phosphorus enrichment of the surface [3, 6–8]. In [6], it has been shown that, in the case of slight anodic polarization, the dissolution of Ni–P coatings is limited to the unsteady bulk diffusion of nickel. The lower rate of dissolution of Ni–P coatings in the region of potentials where nickel is intensely dissolved can be attributed to the barrier action of phosphates [9], nickel oxides with phosphates [10], or a stable amorphous phase [5]. However, the mechanism of anodic dissolution of Ni–P coatings and the causes of the dependence of the corrosion resistance of the coatings on composition and structure have not been conclusively determined.

Recently, Ni–P alloys have been extensively studied as catalytically active materials for electrolytic hydrogen production [11–14]. Analysis of the literature shows that the causes of the catalytic activity of Ni–P alloys in the hydrogen evolution reaction (HER) remain poorly understood. In [11], it is assumed that this activity is determined by the amorphous structure of the coatings; the transition of the amorphous structure of the coatings into a crystalline structure leads to a decrease in the catalytic activity.

In other studies, high catalytic activity of coatings is attributed to the developed surface of the coatings [12] or their ability to absorb a fairly large amount of hydrogen [13]. Absorbed hydrogen changes the electronic structure of the alloys, which affects their catalytic activity in the HER. The author of [13] argues that electrodeposited Ni–P alloys exhibit a higher activity in the HER than alloys prepared by electroless deposition. The catalytic activity of Ni–P alloys is associated with the presence of internal stresses. The authors of [14] state that, in alkali solutions, the catalytic activity of as-deposited Ni–P coatings was slightly lower than that of polycrystalline nickel. In general, the mechanism of the HER on Ni–P coatings has not yet been fully understood.

The corrosion-electrochemical behavior of Ni–P coatings in sulfate media under conditions of natural aeration has been studied previously [15]; in this study, data derived for deaerated sulfate solutions are described and compared to the previous results.

EXPERIMENTAL

Ni–P coatings were deposited at a temperature of 358 ± 1 K from a solution with the following composition, M: $NiCl_2$, 0.127; NaH_2PO_2, 0.114; and CH_3COONa, 0.124; a pH of 3.8–4.9 (pH was adjusted by adding HCl). The phosphorus content in the coatings, which is a function of solution pH (Table 1), was

Table 1. Phosphorus content in the coatings

Solution pH	P content, wt %
4.9	8.0 ± 0.9
4.5	11.1 ± 0.3
3.8	13.4 ± 0.4

determined as described in [16]. The coatings were deposited on samples of Ni foil HO (99.96%). The loading density was ~1.0 dm^2/L; the coating thickness was 15–20 μm.

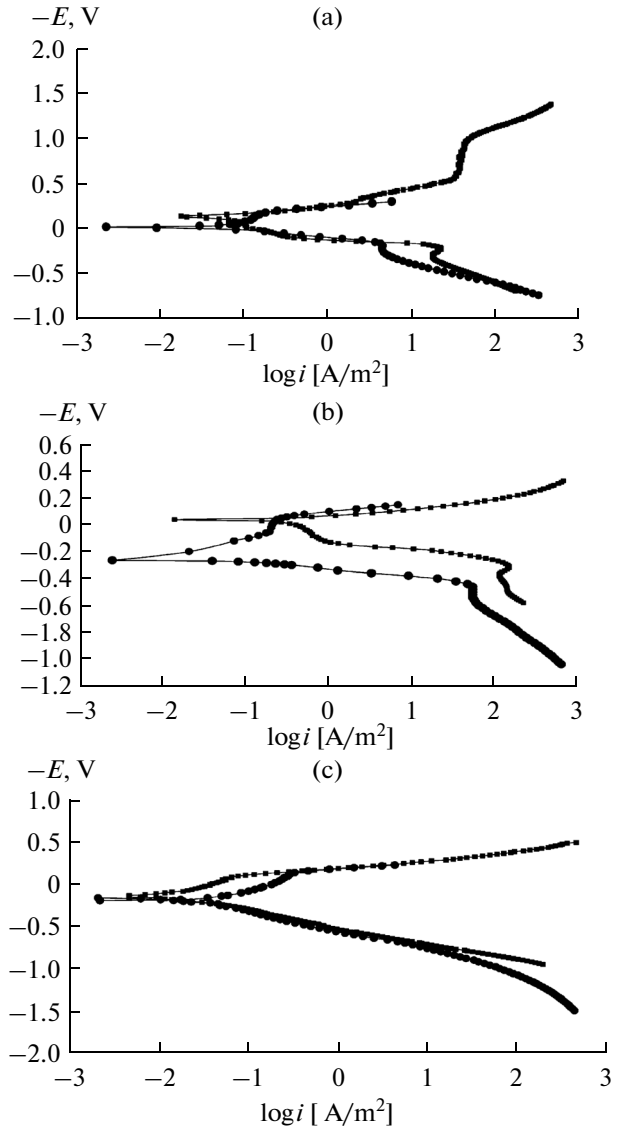

Fig. 1. Polarization curves of the Ni–P coatings in sulfate solutions recorded in (squares) an argon atmosphere and (circles) in the air. The phosphorus content in the coatings: (a, b) 8.0 and (c) 13.4 wt %; the solution pH: (a) 2 and (b, c) 0.5.

Electrochemical studies were conducted in a YaSE-2 standard electrochemical cell in an argon atmosphere and under conditions of natural aeration in a 0.5 M H_2SO_4 solution and in 0.5 M sulfate solutions of $Na_2SO_4 + H_2SO_4$ (with different pH values at a constant ionic strength of the solution). The measurements were conducted using a PI 50-1-1 potentiostat and a PR-8 programming unit. Solutions for the studies were prepared using bidistilled water. Reagent grade Na_2SO_4 was used. The required pH of the sulfate solutions (a pH of 1–3) was adjusted by adding H_2SO_4. The sulfate solutions were prepared using a 0.5 M solution of H_2SO_4 (special purity grade) additionally purified by preliminary electrolysis.

The corrosion-electrochemical studies included potentiodynamic ($v = 5 \times 10^{-4}$ V/s) and chronoamperometric measurements; the rate of corrosion (corrosion current density i_{corr}) was determined by the polarization-resistance method. A silver–silver chloride reference electrode was used; all potentials are given with respect to the NHE. Polarization curves were recorded after holding the electrode in the test solution for 1 h. Under conditions of natural aeration, polarization curves were recorded from free corrosion potential (E_{corr}) to the cathodic and anodic potential regions. In deaerated solutions, polarization curves were recorded moving from the cathodic to the anodic region.

The surface structure and composition of the coatings, as well as changes in the surface composition during anodic polarization, were examined using a Hitachi S-3400N scanning electron microscope equipped with a Bruker energy-dispersive analysis attachment.

EXPERIMENTAL RESULTS AND DISCUSSION

Dissolved oxygen has a significant effect on the rate of corrosion processes even in acidic media because, in addition to the direct involvement of oxygen in the cathodic process, it can be adsorbed on the surface and involved in the formation of surface oxides. To eliminate the effect of dissolved oxygen, potentiodynamic measurements were conducted in an argon atmosphere; to remove oxide films from the surface, a preliminary cathodic polarization was conducted at i_c = 250 A/m^2 by displacing the electrode potential to the cathodic region by ≥0.5 V from the free corrosion potential (E_{corr}) for 5 min.

The polarization curves of the Ni–P coatings in deaerated solutions were compared to the curves measured under conditions of natural aeration (Fig. 1). Comparison of the results shows that the removal of oxygen leads to a shift of E_{corr} to the cathodic region. The magnitude of this shift decreases with an increase in the solution pH and the phosphorus content in the coatings (Tables 2, 3; the data of Table 3 have been

Table 2. Corrosion-electrochemical properties of Ni–P coatings in an argon atmosphere

Corrosive medium	Phosphorus content, wt %	E_{corr}, V	a_c, V	b_c, V	b_{a1}, V	b_{ab}, V	b_{a2}, V	$i_{corr} \times 10^2$, A/m^2*
0.5 M ($Na_2SO_4 + H_2SO_4$), pH 2	8.0	–0.090	0.53	0.09	0.12	0.29	0.05	4.64
	11.1	–0.030	0.54	0.09	0.23	0.34	0.10	1.30
	13.4	0.032	0.54	0.08	0.12	0.68	0.22	0.22
0.5 M ($Na_2SO_4 + H_2SO_4$), pH 1.5	8.0	–0.061	0.32	0.06	0.07	0.22	0.03	6.96
	11.1	0.039	0.39	0.06	0.08	0.19	0.04	1.47
	13.4	0.080	0.49	0.08	0.06	0.34	0.17	0.26
0.5 M ($Na_2SO_4 + H_2SO_4$), pH 1	8.0	–0.039	0.33	0.06	0.14	0.24	0.04	9.26
	11.1	0.087	0.35	0.06	0.13	0.26	0.05	1.57
	13.4	0.115	0.43	0.08	0.09	0.35	0.18	0.85
0.5M H_2SO_4, pH 0.5	8.0	–0.035	0.36	0.06	–	0.31	0.04	21.88
	11.1	0.111	0.43	0.08	–	0.25	0.11	1.70
	13.4	0.140	0.43	0.08	–	0.26	0.22	1.43

* Corrosion currents obtained by extrapolating the Tafel segments.

Table 3. Corrosion-electrochemical properties of Ni–P coatings under conditions of natural aeration

Corrosive medium	P content, wt %	E_{corr}, V	b_{a1}, V	b_{a2}, V	b_{c1}, V	b_{c2}, V	$i_{corr} \times 10^2$, A/m^2*
0.5 M ($Na_2SO_4 + H_2SO_4$), pH 2	8.0	0.004	0.09	0.22	0.09	0.06	2.56
	11.1	0.039	0.13	0.17	0.15	0.07	1.81
	13.4	0.038	0.15	0.18	0.16	0.06	1.38
0.5 M ($Na_2SO_4 + H_2SO_4$), pH 1	8.0	0.082	0.11	0.11	0.12	0.07	3.62
	11.1	0.113	0.14	0.14	0.13	0.06	1.80
	13.4	0.116	0.16	0.21	0.15	0.06	1.83
0.5 M H_2SO_4, pH 0.5	8.0	0.090	0.07	–	0.16	0.06	4.67
	11.1	0.135	0.11	0.16	0.11	0.06	3.02
	13.4	0.205	0.13	0.17	0.13	0.06	2.86

* The i_{corr} values obtained by the polarization-resistance method.

reported previously [15]). In addition, E_{corr} is shifted to the cathodic region because the removal of oxygen from the solution leads to a decrease in the total rate of the cathodic process.

Preliminary cathodic polarization, during which oxide films are removed from the coating surface, results in an additional shift of the polarization curves to the cathodic region (see Fig. 1). This effect is most pronounced for coatings with the lowest phosphorus content in a 0.5 M H_2SO_4 solution (see Fig. 1b).

The main differences in the cathodic curves recorded in air and an argon atmosphere become apparent in close proximity to E_{corr}. At comparable potentials, the cathodic curves recorded in the air are characterized by slightly higher cathodic currents. This fact is associated with the simultaneous occurrence of the cathodic oxygen reduction reaction. An increase in cathodic polarization makes the HER the dominant process; since the contribution of the oxygen reduction reaction is negligible because of the limited solubility of oxygen in solution, the surface oxide films undergo partial reduction.

This fact is responsible for the appearance of the second linear portion in the cathodic E–log$i$ curves. Owing to this, the cathodic curves recorded in both the air and an argon atmosphere almost coincide in this range of potentials (see Fig. 1); the Tafel slopes of the compared portions become close (see Tables 2, 3). Removal of oxygen and preliminary cathodic polarization lead to the extension of the Tafel segments in the cathodic curves.

For the coatings containing 11.1 and 13.4% phosphorus, the corrosion currents in an inert atmosphere are considerably lower (see Tables 2, 3), which is apparently attributed to a decrease in the total rate of the cathodic process. The coatings containing 8.0% phosphorus are characterized by higher i_{corr} values in an inert atmosphere; this is apparently associated with the surface activation of the coatings and the removal of oxide films during preliminary cathodic polarization; in addition, hydrogenation of the coatings should not be ruled out.

Table 2 lists constants a_c and b_c of the Tafel equation. Analysis of the constants shows that an increase in the phosphorus content leads to a decrease in the rate of the HER because the magnitudes of parameters a_c and b_c increase. Hence, coatings with a lower phosphorus content exhibit higher activity in the HER.

The shape of the anodic curves measured in an inert atmosphere is similar to that of the curves recorded in the air. However, the removal of oxygen and preliminary cathodic polarization lead to a significant increase in the anodic dissolution currents of the coatings containing 8.0 and 11.1% phosphorus at comparable potentials. This effect becomes more pronounced with increasing hydrogen ion concentration (for the coatings containing 8.0 and 11.1% phosphorus, the anodic currents increase by 2–2.5 and 1–1.5 orders of magnitude, respectively).

An increase in the anodic currents is mostly associated with the removal of oxide films from the surface and possibly with the hydrogenation of the coatings during preliminary cathodic polarization and the contribution of the ionization current of dissolved hydrogen to the anode current. However, comparison of Figs. 1a and 1b shows that preliminary cathodic polarization in a sulfate solution with a pH of 2 does not lead to an appreciable increase in the anode currents. Furthermore, for the coatings containing 13.4% phosphorus, the anodic curves almost coincide in all the studied solutions regardless of the recording conditions; this is apparently attributed to the fact that these coatings are less prone to forming oxide films and hydrogenation (see Fig. 1c).

In the anodic E–$\log i$ curves, as under conditions of natural aeration, there are short linear portions of dissolution of nickel with a relatively small slope (slopes b_{a1} in Table 2). In some cases, this range of potentials does not exceed 20–40 mV, which complicates the detection of the linear portion. In these cases, b_{a1} values are not listed in Table 2.

After the initial dissolution of the coating, a barrier layer, which is probably enriched in phosphorus, is formed on the coating surface. Owing to this, the dissolution of the coating is complicated and the slope of the curves significantly increases (b_{ab} values in Table 2). Comparison of b_{ab} values suggests that, with an increase in the phosphorus content and the solution pH, these slopes exhibit a tendency to increase.

Further polarization leads to the oxidation of phosphorus accumulated on the surface; this causes the destruction of the barrier layer. In this case, the anodic dissolution currents significantly increase and another linear portion appears in the curves (b_{a2} values in Table 2). In some cases, the b_{a2} values are 0.04–0.05 V (the phosphorus content in the coatings is 8.0 and 11.1%). These slopes are characteristic of the anodic dissolution of nickel. The considerable decrease in the b_{a2} values is attributed to preliminary cathodic polarization and the removal of dissolved oxygen. At the same time, for the coatings containing 13.4% phosphorus, the b_{a2} values are ~0.2 V. Similar processes occur during anodic polarization of the coatings under conditions of natural aeration.

The effect of the pH of the sulfate solution on the corrosion-electrochemical behavior of Ni–P coatings is shown in Fig. 2. The pH range of the studied solutions was based on the fact that, for solutions with pH > 2, during preliminary polarization involving significant cathodic currents, the pH of the original sulfate solution undergoes considerable changes. For the coatings containing 8% phosphorus, a change in the solution pH has a considerable effect on the behavior of the cathodic curves, as evidenced by a substantial increase in the cathodic current with an increase in the acidity of the solution (see Fig. 2a). The effect of pH on the behavior of the anodic curves is less significant and more pronounced in the case of high anodic polarization.

For the coatings containing 11.1% phosphorus, the pH of the sulfate solution has an effect on the behavior of both cathodic and anodic curves. As the acidity increases, at comparable potentials, both the cathodic and anodic currents increase, although the effect of pH on the behavior of the anodic curves is controversial. At the highest phosphorus content in the coatings, pH mostly affects the behavior of the cathodic curves, whereas the anodic curves overlap each other at potentials above 0.2 V (see Fig. 2b).

In the 0.5 M H_2SO_4 solution, an increase in the phosphorus content leads to a decrease in the cathodic reaction rate and the retardation of the anodic dissolution of the coatings. In the sulfate solutions with a pH of 1 and 2 (see Fig. 2c), the phosphorus content is more significant for the anodic behavior of the coatings. In the solution with a pH of 2, the cathodic curves of the coatings almost overlap each other regardless of the phosphorus content; at the same time, with a change in the phosphorus content from 8.0 to 13.4%, the anodic currents decrease by one or two orders of magnitude at comparable potentials (see Fig. 2c).

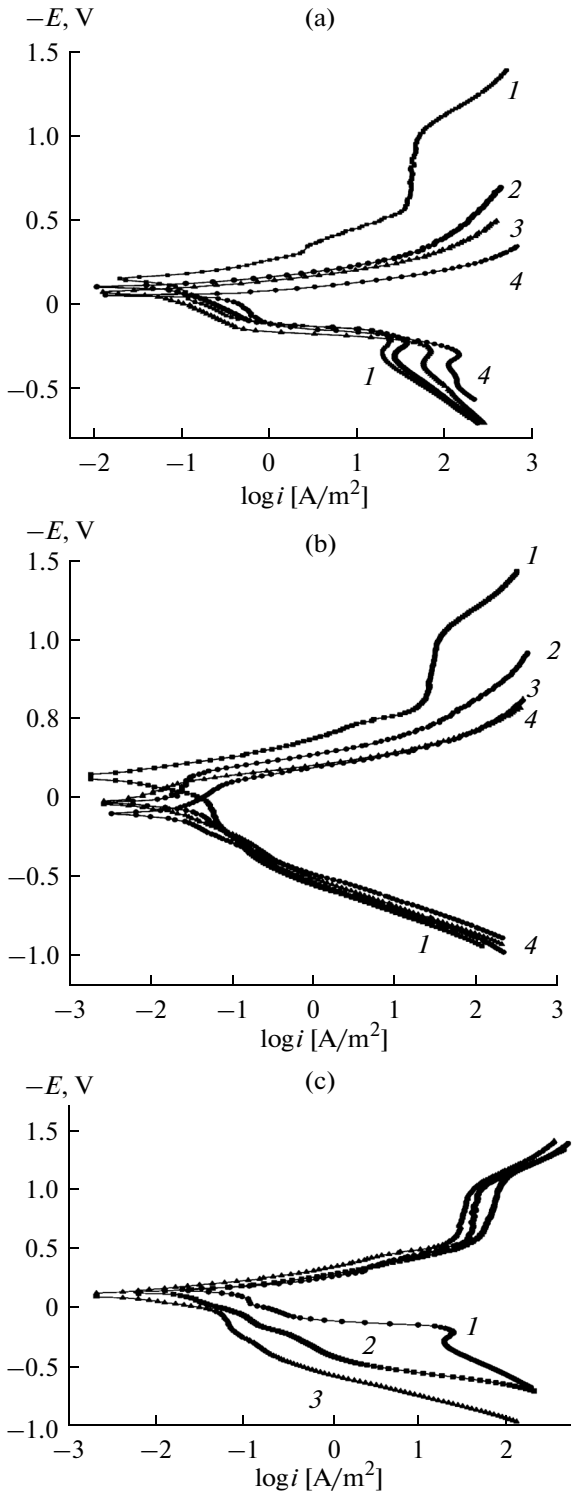

Fig. 2. Polarization curves of the Ni–P coatings in 0.5 M sulfate solutions (a, b) with different pH values ((*1*) 2, (*2*) 1.5, (*3*) 1, and (*4*) 0.5) and (c) with different phosphorus content in the solution with a pH of 2 ((*1*) 8.0, (*2*) 11.1, and (*3*) 13.4%). The phosphorus content: (a) 8.0 and (b) 13.4 wt %.

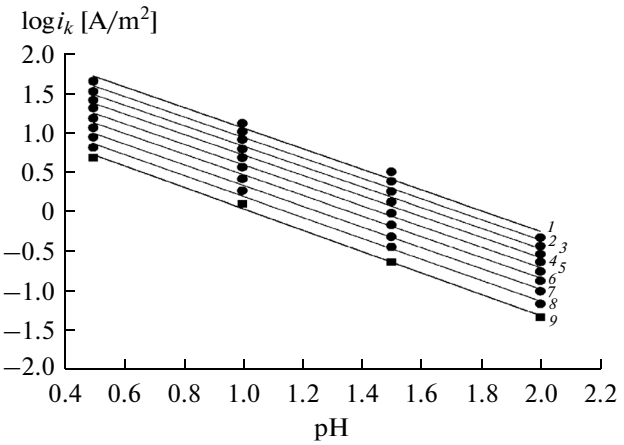

Fig. 3. Dependence of $\log i_c$ on the pH of the sulfate solution for the Ni–P coatings (P content of 11.1 wt %) at different potentials, V: (*1*) 0.25, (*2*) 0.24, (*3*) 0.23, (*4*) 0.22, (*5*) 0.21, (*6*) 0.20, (*7*) 0.19, (*8*) 0.18, and (*9*) 0.17.

The limiting-current area in the cathodic curves in these solutions is determined by a fairly low concentration of hydrogen ions. The discharge of hydrogen ions in the region of the limiting-current area apparently occurs in the diffusion mode. During further cathodic polarization, an increase in the current is caused by the discharge of water molecules.

The polarization curves were processed to derive more information about the kinetics of the cathodic and anodic processes occurring on Ni–P coatings. The processing results are shown in Table 4. Analysis of the results shows that E_{corr} of the coatings containing 11.1% phosphorus exhibits the most significant dependence on pH. These coatings are characterized by a weaker dependence of $\log i_{corr}$ on solution pH. However, of greatest interest are the kinetic characteristics derived for the cathodic reaction, i.e., HER. It should be noted that parameters $\partial E_c/\partial$pH and $\partial\eta_H/\partial$pH are derivatives of coefficient b_c in the Tafel equation and the reaction order with respect to hydrogen ions ($\partial\log i_c/\partial$pH).

The reaction orders for coatings with different phosphorus content were found from the plots, one of which is shown in Fig. 3.

The kinetic dependences were used to reveal the mechanism of the HER. The results suggest that, for the coatings containing 8% phosphorus, coefficient b varies in a range of 0.060–0.062 V. Data derived in the sulfate solution with a pH of 2 are an exception. The reaction order with respect to hydrogen ions is 1.6.

Similar results were obtained for a phosphorus content of 11.1%. In this case, the Tafel slopes are in a range of 0.06–0.077 V. The reaction order is 1.32; that is, it is also close to ~1.5.

It is known that the Tafel slope of ~0.06 V and the order of reaction with respect to hydrogen ions of 1.5 can take place for the discharge–electrochemical desorption route where the rate-limiting step is elec-

Table 4. Kinetic characteristics of the electrode processes on Ni–P coatings in acidic sulfate solutions (pH of 0.5–2)

Phosphorus content, wt %	$-\frac{\partial E_{corr}}{\partial pH}$	$-\frac{\partial \log i_{corr}}{\partial pH}$	$-\frac{\partial E_c}{\partial pH}$	$-\frac{\partial \eta_c}{\partial pH}$	$-\frac{\partial \log i_c}{\partial pH}$
8.0	0.037	0.435	0.109	0.046	1.61
11.1	0.094	0.078	0.091	0.032	1.32
13.4	0.072	0.650	0.094	0.033	1.30

trochemical desorption at surface coverage by adsorbed hydrogen θ of ≈0.5 [17, 18].

For the coatings with a phosphorus content of 13.4%, the Tafel slopes are slightly higher, 0.08 V, while the reaction order with respect to hydrogen ions is 1.3. This value is close to 1.5. It can be assumed that, in this case, the increase in the slope is attributed to the fact that the transfer coefficient differs from 0.5.

Another confirmation of this mechanism is the fact that, with an increase in polarization, a very short Tafel segment with a slope of ~0.12 V is observed on some cathodic curves. In this range of potentials, the reaction order with respect to hydrogen ions is 1. According to [17, 18], these data correspond to the same mechanism (the discharge–electrochemical desorption route where the rate-limiting step is electrochemical desorption) at surface coverage by adsorbed hydrogen $\Theta > 0.5$.

Comparison of the cathodic behavior of Ni–P alloys (coatings) with the cathodic behavior of Ni suggests that the Ni–P coatings, particularly those containing 8% phosphorus, are more efficient cathode materials for the HER in acidic sulfate media than nickel is. It is known [19] that the coefficients of the Tafel equation for the HER for nickel are $a = 0.55$–0.7 V and $b = 0.12$ V. At the same time, for the Ni–P coatings, minimum values of $a = 0.32$–0.34 V and $b = 0.06$ V were obtained.

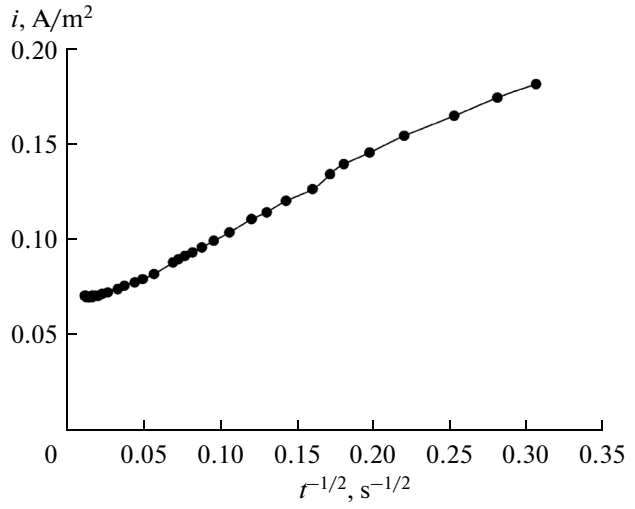

Fig. 4. Chronoamperogram of the Ni–P coating (phosphorus content of 13.4 wt %) in a 0.5 M sulfate solution with a pH of 1 at a potential of 0.242 V.

To confirm the selective dissolution of nickel in the case of a relatively low anodic polarization, chronoamperometric measurements were conducted in acidic sulfate solutions. The formation of a surface film enriched in phosphorus and its compounds complicates the anodic dissolution of coatings. A decrease in the concentration of nickel atoms in the surface layer causes the diffusion of nickel from the layers located at a distance from the coating–solution interface to the surface. After a certain period of time, the dissolution process will be controlled by the diffusion of nickel from the bulk of the coating to the surface.

In this case, the chronoamperograms with the i–$t^{-1/2}$ coordinates exhibit a linear portion, at $t \to \infty$, it is extrapolated to the origin of coordinates or to a certain current value, if the coating is dissolved. In the case of dissolution of the coating, the time dependence of current is expressed by the following equation [20]:

$$i(t) = i_a^{st} + i_b^{st} + \frac{z_a F (C_a^0 - C_a^s) \tilde{D}^{1/2}}{\pi^{1/2} t^{1/2}}, \quad (1)$$

where i_a^{st} and i_b^{st} are the steady-state dissolution rates of the two components of the alloy; $\tilde{D}$ is the interdiffusion coefficient; and C_a^0 and C_a^s are the molar concentrations of component A in the bulk and on the surface, respectively.

For the thickness of the studied coatings (l), the following condition was fulfilled:

$$\frac{l^2}{D_a t} \gg 1. \quad (2)$$

The thickness of the diffusion zone was estimated in accordance with the equation

$$\delta'_{eff} = \frac{\tilde{D}}{V^r}, \quad (3)$$

where V^r is the displacement velocity of the alloy–solution interface.

Chronoamperograms of the coatings containing 13.4% phosphorus were analyzed (Fig. 4). Results of processing of the chronoamperograms in accordance with Eqs. (1) and (3) are shown in Table 5. The dis-

placement velocity of the alloy–solution interface was calculated from the magnitude of the residual anodic current, which results from the extrapolation of the i–$t^{-1/2}$ dependence at $t \to \infty$.

An increase in the pH of the sulfate solution leads to an increase in both the diffusion coefficient and the thickness of the diffusion zone (see Table 5). The residual current decreases with increasing pH; therefore, the increase in the thickness of the diffusion zone with increasing solution pH is more pronounced. The increase in the diffusion coefficient with increasing pH is attributed to an increase in anodic polarization and to a more defective structure of the barrier layer. Apparently, in the case of a lower thickness of the diffusion zone, a fairly large portion of vacancies generated during the dissolution of nickel atoms arrives at the electrode surface and disappears there. A higher dissolution rate results in the formation of a less defective barrier layer.

A significant contribution to the increase in the diffusion coefficient and the thickness of the diffusion zone comes from an increase in anodic polarization. For example, in a sulfate solution with a pH of 1, with a decrease in the anodic polarization from 0.13 to 0.08 V, the diffusion coefficient decreases by almost a factor of 4, while the thickness of the diffusion zone decreases from 62.6 to 32.7 nm. The dependence of the diffusion coefficient on the magnitude of anodic polarization was reported in [21].

Exposure of the coatings to sulfate solutions at a free corrosion potential and low anodic polarization (a shift from E_c by about 0.05–0.1 V) does not lead to a change in the microstructure of the coatings and cracking of the coating surface. According to X-ray microanalysis, after anodic polarization at the above potentials for 1 h, the phosphorus content does not increase. This can be attributed to the fact that the diffusion zone is significantly lower than the thickness of the analyzed layer.

At the same time, studies conducted using a more sensitive technique—X-ray photoelectron spectroscopy—show an increase in the phosphorus content on the surface [21].

Thus, in the case of slight polarization, the anodic dissolution of Ni–P coatings in acidic sulfate solutions can occur by the mechanism of unsteady diffusion of nickel atoms. In this case, a layer enriched in nonmetallic components, mostly atoms and compounds of phosphorus, is formed on the surface. The formation of this layer leads to retardation of the anodic process, which continues until the onset of oxidation of phosphorus with increasing polarization. The surface layer is destroyed, which causes a decrease in the slopes of the E–$\log i$ curves.

Table 5. Parameters of the anodic dissolution of Ni–P coatings (P content of 13.4 wt %) in a sulfate medium

Solution pH	E_a, V	ΔE_a^*, V	$D \times 10^{19}$, m^2/s	$I \times 10^2$, A/m^2	δ, nm
2	0.242	0.198	3.7	3.2	378
1	0.113	0.080	0.27	2.7	33
	0.242	0.129	1.2	6.0	63
0.5	0.273	0.120	0.98	6.9	47

Anodic polarization $\Delta E_a^* = E_a - E_{corr}$.

CONCLUSIONS

(i) It has been found that, with an increase in the phosphorus content in coatings in acidic sulfate media, their activity in the HER decreases. In acidic sulfate media, on Ni–P alloys, the HER occurs via the discharge–electrochemical desorption route, where the rate-limiting step is electrochemical desorption. For Ni–P coatings in sulfate media, low a_c values were obtained, which can be attributed to their electrocatalytic properties with respect to this reaction. Ni–P coatings, particularly those containing 8% phosphorus, are more efficient cathode materials in acidic sulfate media than nickel.

(ii) Preliminary cathodic polarization and an inert atmosphere have little effect on the behavior of the polarization curves of the Ni–P coatings containing 13.4% phosphorus and significantly accelerate the anodic dissolution of the coatings containing 8.0 and 11.1% phosphorus. In the case of slight polarization in acidic sulfate solutions, the anodic dissolution of the coatings can occur by the mechanism of unsteady diffusion of nickel atoms. An increase in the pH of the sulfate solution and anodic polarization leads to an increase in the diffusion coefficients of nickel atoms and the thicknesses of the diffusion zones.

REFERENCES

1. Golovushkina, L.V., Epifanova, V.S., Prusov, Yu.V., and Flerov, V.N., *Elektrokhimiya*, 1974, vol. 10, no. 10, pp. 1526–1529.
2. Salvago, G., Fumagalli, G., and Brunella, F., *Surf. Coat. Technol.*, 1989, vol. 37, no. 4, pp. 449–460.
3. Longfei, Z., Shoufu, L., and Pengxing, L., *Surf. Coat. Technol.*, 1988, vol. 36, nos. 1–2, pp. 455–462.
4. Krolikowski, A. and Pokrywa, B., *Metal. Odlewn.*, 1990, vol. 1, no. 1, pp. 111–117.
5. Krolikowski, A., Karbownicka, B., and Jaklewicz, O., *Electrochim. Acta*, 2006, vol. 51, no. 27, pp. 6120–6127.
6. Petukhov, I.V., Shcherban', M.G., Skryabina, N.E., and Malinina, L.N., *Prot. Met.*, 2002, vol. 38, no. 4, pp. 370–376.
7. Habazaki, H., Ding, S.-Q., Kawashima, A., et al., *Corros. Sci.*, 1991, vol. 32, no. 11, pp. 1227–1235.

8. Zhang, B.-P., Habazaki, H., Kawashima, A., et al., *Corros. Sci.*, 1992, vol. 33, no. 5, pp. 667–679.

9. Flis, J. and Duquette, D.J., *Corrosion*, 1985, vol. 41, no. 12, pp. 700–706.

10. De Lima Neto, P., Rabelo, F.J.B., Adam, A.M.M., et al., *Quim. Nova*, 1996, vol. 19, no. 4, pp. 345–349.

11. Burchardt, T., Hansen, V., and Valand, T., *Electrochim. Acta*, 2001, vol. 46, no. 18, pp. 2761–2766.

12. Krolikowski, A. and Wiecko, A., *Electrochim. Acta*, 2002, vol. 47, nos. 13–14, pp. 2065–2069.

13. Paseka, I., *Electrochim. Acta*, 2008, vol. 53, no. 13, pp. 4537–4543.

14. Abrantes, L.M. and Fundo, A.M., *J. Electroanal. Chem.*, 2007, vol. 600, no. 1, pp. 63–79.

15. Petukhov, I.V. and Medvedeva, N.A., *Corros. Mater. Zashch.*, 2009, no. 7, pp. 27–31.

16. Dymov, A.M., *Tekhnicheskii analiz rud i mineralov* (Engineering Analysis of Ores and Minerals), Moscow: Metallurgizdat, 1949.

17. Brug, G.J., Sluyters-Rehbach, M., and Sluyters, J.H., *J. Electroanal. Chem.,* 1984, vol. 181, nos. 1–2, pp. 245–266.

18. Tilak, B.V. and Chen, C.P., , *J. Appl. Electrochem.*, 1993, vol. 23, no. 6, pp. 631–640.

19. Krishtalik, L.I., *Advances in Electrochemistry and Electrochemical Engineering*, New York: Interscience, 1970, vol. 7, pp. 283–340.

20. Marshakov, I.K., Vvedenskii, A.V., Kondrashin, V.Yu., and Bokov, G.A., *Anodnoe rastvorenie i selektivnaya korroziya splavov* (Anodic Dissolution and Selective Corrosion of Alloys), Voronezh: Voronezh Gos. Univ., 1988.

21. Crobu, M., Scorciapino, A., Elsener, B., and Rossi, A., *Electrochim. Acta*, 2008, vol. 53, no. 8, pp. 3364–3370.

Translated by M. Timoshinina